Subaperture stitching testing of an aspherical surface

Xiaokun Wang（王孝坤）

Key Laboratory of Optical System Advanced Manufacturing Technology，Changchun Institute of Optics，

Fine Mechanics and Physics，Chinese Academy of Sciences，Changchun 130033，*China*

Corresponding author：jimwxk@sohu.com

Abstract　For the purpose to test large and off-axis aspheric surfaces without the aid of other null optics, a novel method combined subaperture stitching and interferometry is introduced. The basic principle and theory of the technique are researched, the synthetical optimization stitching mode and effective stitching algorithm are established based on homogeneous coordinates transformation and simultaneous least-squares fitting. The software of SSI is devised, and the prototype for testing of large aspheres by SSI is designed and developed. The experiment is carried on with three subapertures for an off-axis sic aspheric mirror with a clear aperture of 230×141 （mm）. For the compare and validation, the asphere is also tested by null compensation, the synthesized surface map is consistent to the entire surface map from the null test, the differences of PV and RMS error are 0.023λ and 0.014λ, respectively; and the relative errors of PV and RMS are 0.57% and 2.74%, respectively. The results conclude that this technique is feasible and accurate. It enables the non-null testing of parts with greater asphericity and larger aperture.

OCIS codes　120.0120，120.3180，120.6650，240.0240

doi：10.3788/CJL201239.s108002

1　Introduction

Because the aspherical surfaces permit optical designs and optical systems with fewer elements, resulting in decreased system weight, size, complexity, and cost, as well as increased transmissivity and improved image quality[1-4], they are extremely important in optical systems and have been applied in various kinds of fields. As the use of aspheres in optical systems becomes more and more prevalent, the need for precise and efficient metrology grows. One of the most promising measurement is interferometry[5-7]. Because of its high resolution, high sensitivity and reproducibility, this technology has become the standard tool for testing optical surfaces and wavefronts.

However, when testing the aspheric surfaces with large aperture, steep and large departure, many interference fringes are formed on the detection device and make proper analysis difficult to perform, so we will fall back on auxiliary optics such as null corrector and computer generated hologram (CGH)[8-11]. The auxiliary elements must have been specially designed and customized, it needs much more time and cost, moreover it brings other errors including both manufacturing errors and some unavoidable misalignment errors. The cost of making and verifying the null elements conspires to keep aspheres from practical optical designs.

Subaperture stitching interferometry (SSI) can expand the longitudinal and lateral dynamic ranges of the interferometer, and broaden the scope of measurement significantly[12-15]. The basic idea of subaperture testing method was first proposed by Kim in 1982[16]. It can test large optical system by an array of smaller optical flats without large reference flat, which substantially

reduces the cost and complexity. The second milestone is the discrete phase method developed by Stuhlinger[17]. Then the least-squares method to fit the relative piston and tilt by the datum of overlapping regions was introduced by Otsubo *et al*.[13,18]. The mentioned stitching methods were effective for testing large flats, but they cannot measure large spheres or aspheric surfaces.

Recently, in order to solve the key problems in subaperture testing of aspheric surfaces, Chen established the subaperture stitching algorithms formulated from the geometrical point of view, combined with methods for workpiece localization, tolerance assessment and multi-view registration[19].

The last significant progress of SSI is the automated subaperture stitching interferometer workstation produced by QED (Queues Enforth Development, Inc.) technologies[20-22]. It is applicable not only to plano optics, but also spherical and moderate aspheric surfaces with the aperture smaller than 200 mm. But the mathematic model and stitching algorithm have not been described in detail by QED.

Recently we have proposed a synthetical optimization stitching algorithm for testing large and off-axis aspheric surfaces by SSI[23,24]. In this letter, a prototype for testing of large aspheres by SSI is developed, it can test large aperture aspheric surfaces at high resolution, low cost, and high efficiency without any null optics.

2　Basic Theory And Process

The sketch of the SSI is shown in Fig.1, and the elaborate flow chart is given in Fig.2.
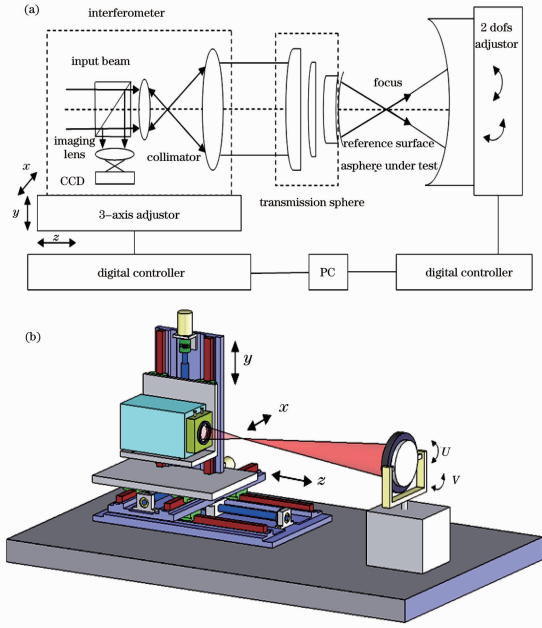
Firstly, we define the surface to be meas-

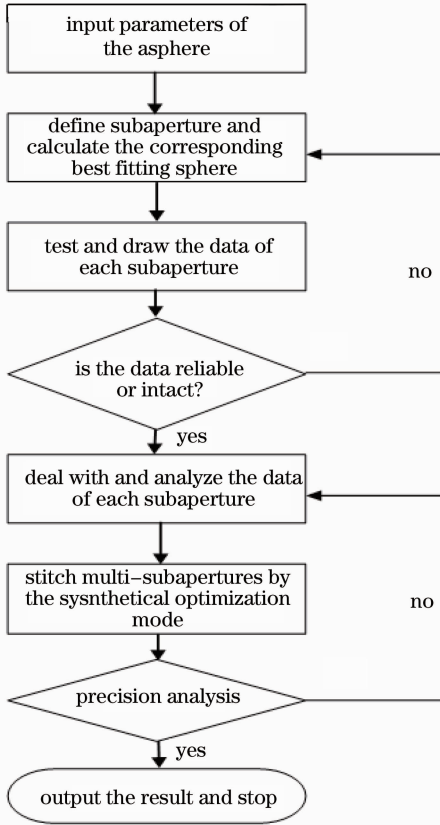Fig.1. (a) Sketch of setup and (b) model for testing asphere by SSI

Fig.2. Flow chart of SSI

ured, in particular its nominal aperture and radius of the curvature. The proper transmission sphere is selected correctly, then the size and number of the subaperture is determined by the surface diameter and the relative aperture.

The second step is to control the interferometer

and the tested asphere precisely, the first null is located at the center of the surface, the curvature of the spherical wavefront is consistent with the measured region, the phase distribution of this region will be recorded.

Thirdly, we align the interferometer or the asphere again and again, let the slope of the spherical wavefront match the slope of the outer subaperture and make the adjacent subapertures have some overlapping areas, then the phase data of each subaperture is acquired by interferometric method, and the data of the corresponding subaperture will be recorded.

Fourthly, we choose the subaperture in the center region of the aspheric surface for the fiducial subaperture, the data of all the subapertures will be unified into the same reference by homogeneous coordinates transformation, and the relative translation error will be eliminated from each subaperture through the simultaneous least-squares method by minimizing the discrepancy in the overlapping areas.

After all the translation errors have been subtracted, a final least-squares fitting is performed to evaluate the misalignment errors of the whole system.

3　Stitching Algorithm

The phase data of each subaperture can be obtained by interferometry, then the data of all the subapertures can be unified into the same reference by homogeneous coordinates transformation.

Sketch of SSI is given in Fig. 3. Supposing the difference of the same point in the overlapping area between the adjacent subaperture is W_A, W_A is introduced by the rigid-body motion of the off-axis mirror and should be removed from the result. The rigid-body has six freedom degrees, it contains D_x, D_y, D_z and x, y, z, where D_x, D_y, D_z are the displacements of the entire conic section, and θ_x, θ_y, θ_z are rotations about these parent coordinate axis, θ_z is of no significance here (due to rotational symmetry of parent about its axis)[25].
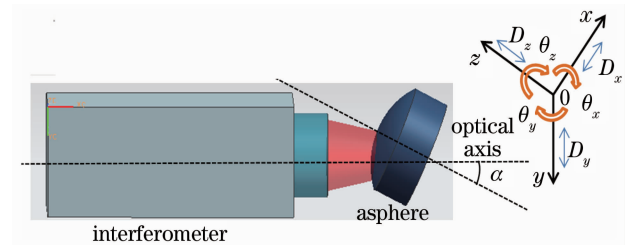

Fig.3. Sketch of SSI

The wavefront change $W_A(x, y)$ associated with the vector displacement $\boldsymbol{\delta}_d$ of any point on the surface is given by

$$W_A(x,y) = -2(\boldsymbol{\delta}_d \cdot \boldsymbol{n}),\qquad(1)$$

where $\boldsymbol{n}$ is unit vectors along the normal to the surface. For a general conic section, with $k = 1-e^2$ and vertex curvature $c = 1/R$, we can find the following

terms

$$W_A = -\underset{\text{Piston}}{2D_z} + 2x(cD_x + \theta_y) + 2y(cD_y - \theta_x) +$$
$$\underset{\text{Defocus}}{p^2 c^2 D_z} + \underset{x\text{ Coma}}{xp^2(kc^3 D_x)} + \underset{y\text{ Coma}}{yp^2(kc^3 D_y)} +$$
$$\underset{\text{Spherical}}{p^4 \frac{(1+4k)c^4}{8} D_z}. \qquad (2)$$

For on-axis optical system, we can see the main misalignment-induced aberrations are tilt, focus, coma, and spherical. But for off-axis aspherical optical system ,we wish to express the wavefront aberrations in terms of subaperture coordinates, Eq. (2) has changed to the following terms

$$W_A(x,y) = -2D_z + \underset{\text{Piston}}{2cx_c D_x} + 2cy_c Dy - 2y_c \theta_x + 2x_c \theta_y +$$
$$\underset{x\text{ tilt}}{(2cD_x + 2\theta_y)x_x} + \underset{y\text{ tilt}}{(2Cd_y - 2\theta_x)Y_x} + \underset{\text{Focus}}{p_s^2 c^2 D_z} + x_c p_s^2 c^3 kD_x + y_c p_s^2 c^3 kD_y + s^2 p_s^2 c^4 \frac{4k+1}{8}D_z +$$
$$\underset{\text{Astigmatism}}{2x_c x_s^2 c^3 kD_x} + 2y_c x_s y_s c^3 kD_s + 2x_c x_s y_s c^3 kD_y + 2y_c y_s^2 c^3 kD_y + x_c^2 x_s^2 c^4 \frac{4k+1}{2}D_z + y_c^2 y_s^2 c^4 \frac{4k+1}{2}D_z +$$
$$\underset{\text{Coma}}{x_c x_s y_c y_s c^4(4k+1)D_z} + x_s p_s^2 c^3 kD_s + y_s p_s^2 c^3 kD_y + x_c x_s p_s^2 c^4 \frac{4k+1}{2}D_z +$$
$$\underset{\text{Spherical}}{y_c y_s p_s^2 c^4 \frac{4k+1}{2}D_z} + p_s^4 c^4 \frac{4k+1}{8}D_z. \qquad (3)$$

We can stitch two subapertures by subtracting the translation errors of adjacent subapertures. Using the principle of two subapertures splicing many times may realize multi-subaperture stitching. But it often brings the erroneous transmission and accumulation, thus the precision will be reduced.

In this letter, the sum of the squared differences for all common areas should be minimized simultaneously. Suppose there are M subapertures altogether. In order to be simple for the localization and measurement, generally choosing the subaperture in the central region of the aspheric surface for the fiducial subaperture, it can be seen from Eq. (3), the misalignment of adjacent subapertures will have combinations of different amount of piston, tilt, power, astigmatism,coma, and primary spherical. So each measurement needs to hold the following function for the correction of piston, tilt , power, astigmatism, coma, and primary spherical:

$$W_0 = W_1 + p_1 + a_1 x_1 + b_1 y_+ c_(x_1^2 + y_1^2) + d_1 x_1 y_1 + e_1(x_1^2 - y_1^2) +$$
$$f_1 x_1(x_1^2 + y_1^2) + g_1 y_1(x_1^2 + y_1^2) + h_1(x_1^2 + y_1^2)^2 =$$
$$W_2 + p_2 + a_2 x_2 + c_2(x_2^2 + y_2^2) + d_2 x_2 y_2 + e_2(x_2^2 - y_2^2) + f_2 x_2(x_2^2 + y_2^2) + g_2 y_2(x_2^2 + y_2^2) + h_2(x_2^2 + y_2^2)^2 \vdots =$$
$$W_{M-1} + p_{M-1} + a_{M-1} x_{M-1} + b_{M-1} y_{M-1} + c_{M-1}(x_{M-1}^2 + y_{M-1}^2) + d_{M-1} x_{M-1} y_{M-1} + e_{M-1}(x_{M-1}^2 - y_{M-1}^2) +$$
$$f_{M-1} x_{M-1}(x_{M-1}^2 + y_{M-1}^2) + g_{M-1} y_{M-1}(x_{M-1}^2 + y_{M-1}^2) + h_{M-1}(x_{M-1}^2 + y_{M-1}^2), \qquad (4)$$

where W_0 is the phase distribution of the fiducial subaperture, $W_1, W_2, \cdots, W_{M-1}$ are the phase distributions of other subapertures, p_i, a_i, b_i, c_i are the coefficients of the relative translation errors to the fiducial subaperture of the displacement, tilt in the x and y directions and power respectively, d_i, e_i are the coefficients of the relative astigmatism, and f_i, g_i are the coefficients of the relative coma, h_i is the coefficients of the relative primary spherical.

By using least squares fitting derived to minimize the sum of the squared differences in the all overlapping regions, as

$$S = \sum_{j_1 \neq 0 i_1 \subset W_0, W_{j_1}}^{N_1} \sum^{n} \{W_0(x_{0i_1}, y_{0i_1}) - [W_{j_1}(x_{j_1 i_1}, y_{j_1 i_1}) + p_{j_1} x_{j_1 i_1} + a_{j_1} x_{j_1 i_1} + b_{j_1} y_{j_1 i_1} + c_{j_1}(x_{j_1 i_1}^2 + y_{j_1 i_1}^2) +$$
$$d_{j_1} x_{j_1 i_1} y_{j_1 i_1} + e_{j_1}(x_{j_1 i_1}^2 - y_{j_1 i_1}^2) + f_{j_1} x_{j_1 i_1}(x_{j_1 i_1}^2 + y_{j_1 i_1}^2) + g_{j_1} y_{j_1 i_1}(x_{j_1 i_1}^2 +$$
$$y_{j_1 i_1}^2) + h_{j_1}(x_{j_1 i_1}^2 + y_{j_1 i_1}^2)^2]\}^2 + \sum_{j_2 \cap j_3 \neq 0 i_2 \subset W_{j_2}, W_{j_3}}^{N_2} \sum^{n} \{[W_{j_2}(x_{j_2 i_2}, y_{j_2 i_2}) + p_{j_2} x_{j_2 i_2} + a_{j_2} x_{j_2 i_2} + b_{j_2} y_{j_2 i_2} +$$
$$c_{j_2}(x_{j_2 i_2}^2 + y_{j_2 i_2}^2) + d_{j_2} x_{j_2 i_2} y_{j_2 i_2} + e_{j_2}(x_{j_2 i_2}^2 - y_{j_2 i_2}^2) + f_{j_2} x_{j_2 i_2}(x_{j_2 i_2}^2 + y_{j_2 i_2}^2) + g_{j_2} y_{j_2 i_2}(x_{j_2 i_2}^2 + y_{j_2 i_2}^2) +$$
$$h_{j_2}(x_{j_2 i_2}^2 + y_{j_2 i_2}^2)^2] - [W_{j_3}(x_{j_3 i_2}, y_{j_3 i_2}) + p_{j_3} x_{j_3 i_2} + a_{j_3} x_{j_3 i_2} + b_{j_3} y_{j_3 i_2} + c_{j_3}(x_{j_3 i_2}^2 + y_{j_3 i_2}^2) + d_{j_3} x_{j_3 i_2} y_{j_3 i_2} +$$
$$e_{j_3}(x_{j_3 i_2}^2 - y_{j_3 i_2}^2) + f_{j_3} x_{j_3 i_2}(x_{j_3 i_2}^2 + y_{j_3 i_2}^2) + g_{j_3} y_{j_3 i_2}(x_{j_3 i_2}^2 + y_{j_3 i_2}^2) + h_{j_3}(x_{j_3 i_2}^2 + y_{j_3 i_2}^2)^2]\}^2 = \min, \qquad (5)$$

where (x_{1i_1}, y_{1i_1}), $(x_{j_1 i_1}, y_{j_1 i_1})$, $(x_{j_2 i_2}, y_{j_2 i_2})$, and $(x_{j_3 i_2}, y_{j_3 i_2})$ denote spatial coordinate system of the unified reference coordinates of each subaperture; N_1 is the number of subapertures overlapping the fiducial; N_2 is the number of subapertures overlapping other subaperture, excluding the fiducial subaperture; n is the number of sampling points of each common region, the total number of the overlapping areas is $N_1 + N_2$.

Taking the differentiations of Eq. (5) with respect to these unknows, the least squares equation can be described as Eq. (6), where i is integer from 1 to $M-1$, then the best splicing parameters can be obtained by this function, so the phase data of all the subapertures can be unified to the same benchmark.

We choose the central subaperture for the fiducial subaperture, and make data of all the subapertures unify into the same reference by homogeneous coordinates transformation, then eliminate the relativetranslation error from each subaperture using the simultaneous least-square method by minimizing the discrepancy in the overlapping areas.

The coordinate frame of the subaperture is shown in Fig. 4, where (x_0, y_0, W_0) is the coordinate frame of the fiducial subaperture while (x_i, y_i, W_i) is the coordinate of other subapertures.

$$\begin{cases} \dfrac{\partial S}{\partial p_i} = 0 \\ \dfrac{\partial S}{\partial a_i} = 0, \\ \dfrac{\partial S}{\partial b_i} = 0 \end{cases} \begin{cases} \dfrac{\partial S}{\partial c_i} = 0 \\ \dfrac{\partial S}{\partial d_i} = 0, \\ \dfrac{\partial S}{\partial e_i} = 0 \end{cases} \begin{cases} \dfrac{\partial S}{\partial f_i} = 0 \\ \dfrac{\partial S}{\partial g_i} = 0. \\ \dfrac{\partial S}{\partial h_i} = 0 \end{cases} \quad (6)$$

According to homogeneous coordinates transformation, the relationship between them can be
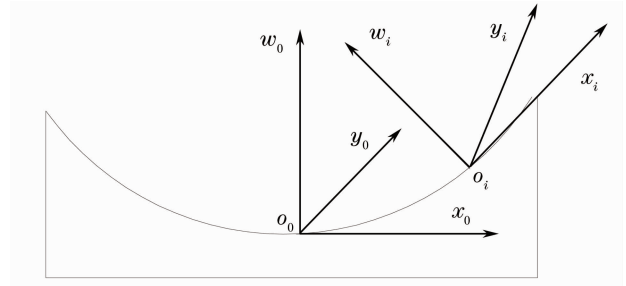

Fig. 4. Coordinate of the subaperture

expressed as

$$(x_0, y_0, W_0, 1) = (x_i, y_i, W_i, 1) \cdot V, \quad (7)$$

where V is the transpositional matrix that can be described as

$$V = T \cdot R \cdot S, \quad (8)$$

where T is the matrix of translation. Supposing the relative translations to the fiducial subaperture in the x, y, and W directions are P_x, P_y, and P_w, respectively, it can be expressed as

$$T = T_x \cdot T_y \cdot T_w = \begin{bmatrix} 0 & 0 & 0 & 0 \\ 0 & 1 & 0 & 0 \\ 0 & 0 & 1 & 0 \\ P_x & 0 & 0 & 1 \end{bmatrix} \times$$

$$\begin{bmatrix} 1 & 0 & 0 & 0 \\ 0 & 1 & 0 & 0 \\ 0 & 0 & 1 & 0 \\ 0 & P_y & 0 & 1 \end{bmatrix} \begin{bmatrix} 1 & 0 & 0 & 0 \\ 0 & 1 & 0 & 0 \\ 0 & 0 & 1 & 0 \\ 0 & 0 & P_w & 1 \end{bmatrix} =$$

$$\begin{bmatrix} 1 & 0 & 0 & 0 \\ 0 & 1 & 0 & 0 \\ 0 & 0 & 1 & 0 \\ P_x & P_y & P_w & 1 \end{bmatrix}, \quad (9)$$

R in Eq. (5) is the matrix of rotation. Supposing the relative rotations to the fiducial subaperture in the x, y, and W directions are α, β, and γ, respectively, it can be expressed as

$$R = R_x \cdot R_y \cdot R_w = \begin{bmatrix} 1 & 0 & 0 & 0 \\ 0 & \cos\alpha & \sin\alpha & 0 \\ 0 & -\sin\alpha & \cos\alpha & 0 \\ 0 & 0 & 0 & 1 \end{bmatrix} \begin{bmatrix} \cos\beta & 0 & -\sin\beta & 0 \\ 0 & 1 & 0 & 0 \\ \sin\beta & 0 & \cos\beta & 0 \\ 0 & 0 & 0 & 1 \end{bmatrix} \begin{bmatrix} \cos\gamma & \sin\gamma & 0 & 0 \\ -\sin\gamma & \cos\gamma & 0 & 0 \\ 0 & 0 & 1 & 0 \\ 0 & 0 & 0 & 1 \end{bmatrix} =$$

$$\begin{bmatrix} \cos\beta\cos\gamma & \cos\beta\sin\gamma & -\sin\beta & 0 \\ \sin\alpha\sin\beta\cos\gamma - \cos\alpha\sin\gamma & \sin\alpha\sin\beta\sin\gamma + \cos\alpha\cos\gamma & \sin\alpha\cos\beta & 0 \\ \cos\alpha\sin\beta\cos\gamma + \sin\alpha\sin\gamma & \cos\alpha\sin\beta\sin\gamma - \sin\alpha\cos\gamma & \cos\alpha\cos\beta & 0 \\ 0 & 0 & 0 & 1 \end{bmatrix}, \quad (10)$$

Because the asphere under test is rotational-symmetric, γ is equal to zero. S is the matrix of scale. Because the zoom of CCD is the same to each subaperture, S is set 1.

Hence the phase data of all the subapertures can be unified to the same benchmark and stitched together by Eqs. (6)-(10).

After all the relative translation errors are eliminated, a least-squares fitting is implemented to evaluate the misalignment errors of the system as

$$\sum_{i=1}^{N} \{ \Phi_i(x_i, y_i) - [Ax_i + By_i + C(x_i^2 + y_i^2) + D] \}^2 = \min, \quad (11)$$

where Φ_i is the phase distribution over the full

aperture； N is the number of total sampling points； A,B,C,D are the misalignment coefficients

that can be obtained by

$$\begin{bmatrix} A \\ B \\ C \\ D \end{bmatrix} = \begin{bmatrix} \sum xx & \sum xy & \sum x(x^2+y^2) & \sum x \\ \sum yx & \sum yy & \sum y(x^2+y^2) & \sum y \\ \sum (x^2+y^2)x & \sum (x^2+y^2)y & \sum (x^2+y^2)^2 & \sum (x^2+y^2) \\ \sum x & \sum y & \sum (x^2+y^2) & N \end{bmatrix}^{-1} \begin{bmatrix} \sum x\Phi \\ \sum y\Phi \\ \sum (x^2+y^2)\Phi \\ \sum \Phi \end{bmatrix}. \quad (12)$$

So we can obtain the accurate figure error of the asphere by removing these errors.

We have desived the primary software of SSI, the interface of algorithm for SSI is shown in Fig. 5. By this stitching algorithm and software we can test aspherical surfaces swiftly without other assistant optics[26,27].
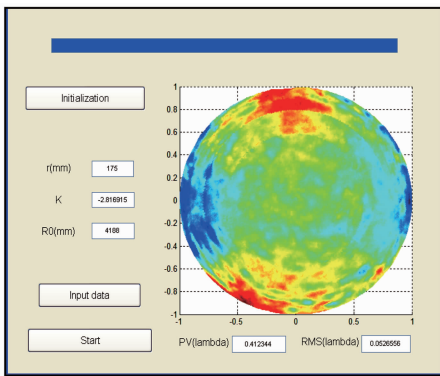
Fig. 5. Interface of algorithm for SSI

4　Experiment

We have tested a hyperboloid to verify the proposed mathematical model and the stitching algorithm. The tested asphere with a clear aperture of 230×141 (mm) and a radius of curvature at the vertex of approximately -1359.81 mm，the conic constant is -1.60，and the off-axis quantity is -89.50 mm. The experimental setup is showed in Fig. 6.
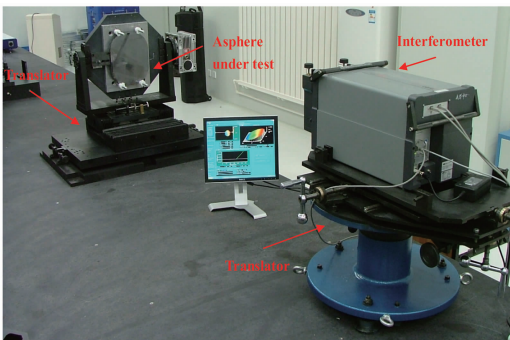

Fig. 6. Setup of the stitching interferometry

There are a total of 5 dofs to align and null the interferometer or the subaperture. The Zygo interferomer is mounted on a $x/y/z$ translation stage. The tested asphere is mounted on a three axes stage，which can adjust the tip，tilt and defocus of the asphere precisely. The whole setup is mounted on a vibration isolator. A lattice design that achieves coverage of the asphere with three subapertures is illustrated in Fig. 7，the subaperture is about sixty percent of the full aperture. By aligning the interferometer and the tested asphere，placing radius of the best-fitting sphere of each subaperture coincident with the focus of the transmission sphere，the test beam can retrace in the same way approximately，the reference beam and test beam may form a interferogram. The result of the three individual measurements is given in Fig. 8.
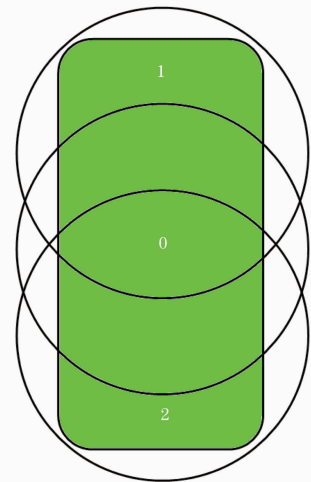

Fig. 7. Distribution of subapertures

Then all the subapertures can be unified into the same standard by homogeneous coordinates transformation，and the translation error can be eliminated from each subaperture by using the simultaneous least-squares method. After all the translations errors have been removed，a final least-squres fitting is performed to evaluate the misalignment errors of the whole system，the misalignment coefficients of tilt in the x and y directions，power and piston are $0.0012756, -0.0186697, 0.0101530$, and -0.0074929, respectively. We can obtain the exact figure error of the asphere by eliminating these errors. The surface map of the full aperture reconstructed by the stitching method is given in Fig. 9，where the PV error is 4.087λ and RMS error is 0.525λ. Because of the random noise，the slight systemic error and the tiny misalignment errors between the adjacent subapertures，the stitched map is noisy shaped.
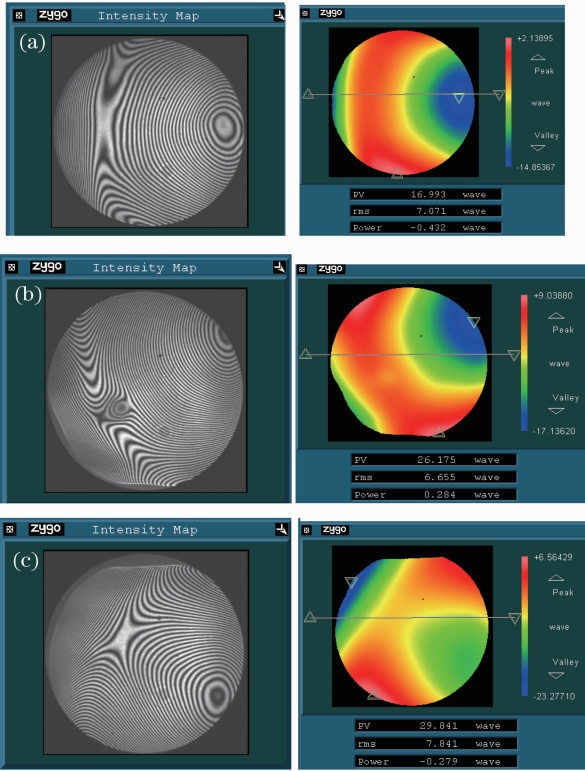
Fig. 8. Corresponding interferograms and phase distributions of three subapertures

PV: 4.087 λ　　　　RMS: 0.525 λ

(b)

Fig. 9. Normalized surface map of the whole aperture after stitching

Fig. 10. Sketch of testing aspheric surface by offner null compensator

In order to contrast and validate，we have designed an offner null corrector to test the aspherical surface，the sketch of testing aspheric surface by offner null compensator is given in Fig. 10. The null corrector can introduce enough aberration（of the opposite sign）into the test beam so that it eliminates the aberration produced by testing the aspheric surface at its center of curvature[28-30]. It consists of two positive piano-convex lenses：the field and relay lenses. Both lenses are located near the center of curvature of the mirror under test，so they are significantly smaller than the test mirror itself. The function of the field lens is to rearrange in a linear way the rays that arrive to the relay lens. The function of the relay lens is to introduce the bulk of the optical correction and to obtain a null test point.

The phase map from the null test are given in Fig. 11，where the PV and RMS are 4.064λ and 0.511λ, respectively. Note that，the differences of PV and RMS error between the two methods are 0.023λ and 0.014λ, respectively；and the relative errors of PV and RMS are 0.57% and 2.74%, respectively. Furthermore，the PV and RMS of residual error of phase distribution of these two methods are calculated. The map of the residual error is given in Fig. 12，where PV $(\delta w) = 0.136\lambda$, RMS$(\delta w) = 0.018\lambda$. Because the datum and the sample density of the two methods are different，the tiny differences of the testing results are reasonable and acceptable.
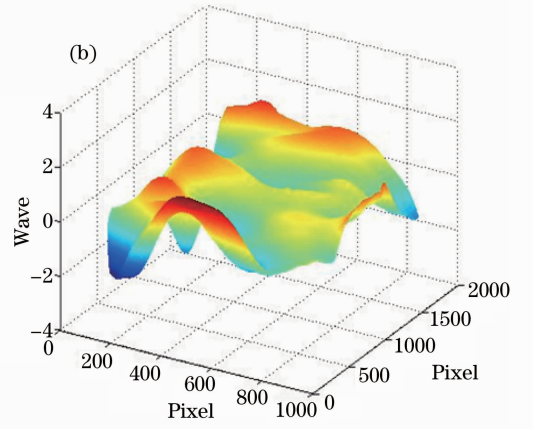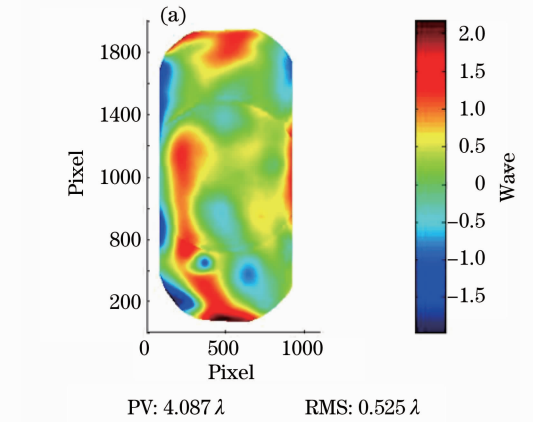
Because the asphere has been polished for a short time，the surface map is not well，we will do the SSI when the surface error is very tiny. But the results conclude that SSI is feasible and accurate. Although only three subapertures were required to cover the full aperture in this experiment，the same stitching procedure can be extended to test those larger and deeper aspherical surfaces with more subapertures.

5　Conclusion

In conclusion，a novel method for testing large aspherical surfaces by subaperture stitching interferometry is proposed and introduced. It expands the longitudinal and lateral dynamic ranges of interferometer，and
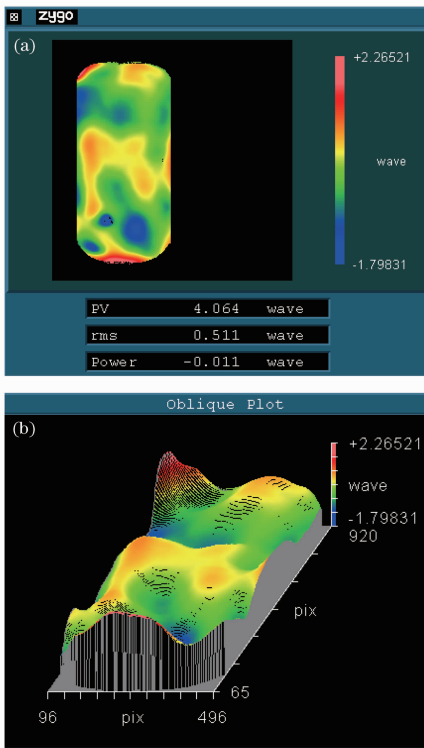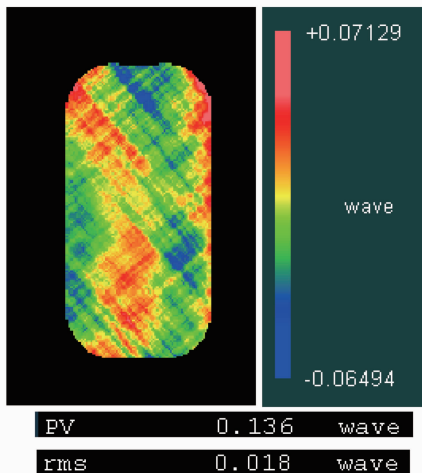
Fig. 11. Surface map from null compensation

Fig. 12. Residual error between SSI and null test

broadens the scope of measurement significantly. We utilizes the synthetical optimization stitching mode, the stitching algorithm is based on a simultaneous least-squares minimization the mismatch among all overlapping regions, it prevents the error from transmitting and accumulating. The physical concept of this method is simple and clear, data processing and mathematical operation are convenient. An off-axis aspherical mirror with the aperture of 230×141 (mm) is tested by this method, and we apply SSI to the practical engineering. The results of the experiment conclude that this mathematical mode and stitching algorithm are feasible and effective. This technology has a wide scope of application, it can test large flat and sphere, large asphere,

high numerical aperture asphere, convex aspheric surface even for freeform optics. Moreover, this technology can test random region of the surface, so it offers a guarantee for ultra-precise fabrication and measurement. The final accuracy of the SSI depends on a series of factors including the precision of location of subapertures, the data acquisition and data reduction processes, the precision of algorithm, and a variety of environmental efforts, etc, we will analyse and research these problems in the future.

References

1 H. Kurita, K. Saito, and M. Kato, Proc. SPIE **680**, 47 (1986).

2 D. Malacara, Optical Shop Testing (J. Wiley & Sons, New York, 1992).

3 R. B. Huxford, Proc. SPIE **5249**, 230 (2004).

4 X. Zhang, Z. Li, and Z. Zhang, Infrared and Laser Engineering (in Chinese) **36**, 192 (2007).

5 S. O´Donohue, G. Devries, P. Murphy, and G. Forbes, Proc. SPIE **5869**, 58690T (2005).

6 M. Wang, Proc. SPIE **4927**, 673 (2002).

7 T. Yatagai, Opt. Eng. **23**, 357 (1984).

8 H. Liu, Z. Lu, and F. Li, Opt. Express **12**, 4348 (2005).

9 J. H. Burge, Proc. SPIE **2576**, 258 (1995).

10 J. B. Song and Y. W. Lee, Proc. SPIE **6034**, 60341M (2006).

11 X. Zhang, Proc. SPIE **4231**, 24 (2000).

12 J. E. Negro, Appl. Opt. **23**, 1921 (1984).

13 O. Masashi, O. Katsuyuki, and T. Jumpei, Opt. Eng. **33**, 608 (1994).

14 S. Aric, K. William, and T. Marc, Proc. SPIE **5494**, 81 (2004).

15 J. Fleig, P. Dumas, P. E. Murphy, and G. W. Forbes, Proc. SPIE **5188**, 296 (2003).

16 C. J. Kim, Appl. Opt. **21**, 4521 (1982).

17 T. W. Stuhlinger, Proc. SPIE **656**, 118 (1986).

18 O. Masashi and O. Katsuyuki, Proc. SPIE **1720**, 444 (1992).

19 S. Chen, "Geometrical Approach to Subaperture Stitching Interferometry for Aspheric Surface", PhD. Thesis (National University of Defense Technology, 2006).

20 M. Tricard, A. Shorey, B. Hallock, and P. Murphy, Proc. SPIE **6273**, 62730L (2006).

21 P. Murphy, J. Fleig, and G. Forbes, Proc. SPIE **6293**, 62930J (2006).

22 M. Tricord, P. Dumas, and G. Forbes, Proc. SPIE **5638**, 284 (2005).

23 X. K. Wang, L. H. Wang, and X. J. Zhang, Optics and Precision Engineering(in Chinese) **15**, 192 (2007).

24 P. E. Murphy, J. Fleig, G. Forbes and M. Tricard, Proc. SPIE **5786**, 113 (2005).

25 D. Xue, L. Zheng, and X. Zhang, Proc. SPIE **5638**, 752 (2005).

26 X. Wang, "Research on the technique for testing of aspheric surfaces by subaperture stitching interferometry", PhD. Thesis (Changchun Institute of Optics, Fine Mechanics and Physics, 2008).

27 X. Wang，L. Zheng，and B. Zhang，Proc. SPIE **7283**，72832J（2009）.

28 P. Guo and J. Yu，Proc. SPIE **6150**，259（2006）.

29 J. M. Sasian，S. A. Lerner，and J. H. Burge，Proc. SPIE **3739**，444（1999）.

30 P. Beraud，J. Espiard，and R. Geyl，Proc. SPIE **2536**，413（1995）.